Decay channels of core-excited HCl

H. Aksela, S. Aksela, M. Ala-Korpela, and O-P. Sairanen
Department of Physics, University of Oulu, SF-90570 Oulu, Finland

M. Hotokka
Department of Physical Chemistry, Åbo Akademi, SF-20500 Åbo, Finland

G. M. Bancroft and K. H. Tan
Department of Chemistry and Center for Chemical Physics, University of Western Ontario, London, Ontario, Canada N6A 5B7
and Canadian Synchrotron Radiation Facility, Synchrotron Radiation Center, University of Wisconsin, Stoughton, Wisconsin 53589

J. Tulkki
Laboratory of Physics, Helsinki University of Technology, SF-02150 Espoo, Finland
(Received 1 May 1989; revised manuscript received 11 December 1989)

The HCl $2p_{Cl} \rightarrow \sigma^*$ photoexcitation resonance has been studied using a tunable synchrotron radiation beam with a narrow bandwidth. Extensive *ab initio* molecular and atomic calculations have been carried out to analyze the details of the measured electron spectra. The interatomic potential-energy curves have been calculated for the ground and selected excited states of HCl using the complete-active-space self-consistent-field method. Multiconfiguration Dirac-Fock energies and line intensities of the atomic chlorine Auger spectrum have been used to identify the intense atomic spectral lines in the measured electron spectrum. Comparison between theory and experiment indicates fast neutral dissociation of the excited HCl molecules, followed by resonance Auger processes of the core-excited chlorine atoms. The atomic spectral lines are found to overlap with a strong background of broad structures, which sum up to 40% of the total intensity. This contribution has been addressed to the 2.9-eV potential well in our potential-energy curve of the excited HCl allowing for Franck-Condon transitions to bound vibrational states with a molecular nonradiative decay mode.

INTRODUCTION

Molecular states having one of the core electrons excited to the first empty molecular orbital are often characterized by absorption bands which are much broader than the natural width of the core hole. This broadening is related to a fast dissociation of the excited molecular state cascading with an atomic decay of the dissociation products.[1-3] As demonstrated recently by Morin and Nenner,[1] synchrotron-radiation excited-electron spectroscopy and mass spectroscopy provide powerful tools to study the decay channels of these resonance states.

In their study of the HBr $3d_{Br} \rightarrow \sigma^*$ excitation Morin and Nenner found evidence of the fast dissociation followed by atomic Auger emission.[1] Their interpretation of the electron spectra was, however, based on a schematic model of the decay sequence and thus excluded any closer study of possible competing decay modes.

In this work we have measured the analogous HCl $2p_{Cl} \rightarrow \sigma^*$ photoexcitation resonance. We have also carried out extensive *ab initio* molecular and atomic calculations in order to find out whether the high-resolution electron spectra can be used to study the details of the pertinent excited molecular states.

EXPERIMENT

The energy of the incoming radiation beam was tuned across the $2p_{Cl} \rightarrow \sigma^*$ resonance and the spectra of emitted electrons were recorded by the Leybold-Heraeus electron spectrometer at the Canadian Synchrotron Radiation Facility located at the 1-GeV Aladdin storage ring.[4] The measured electron spectra are shown in Figs. 1 and 2. The beam line uses the Grasshopper Mark IV grazing incidence monochromator[5] equipped with a 900-groove/mm holographic grating. Most spectra were taken applying a constant 50 eV pass energy in the electron spectrometer and the monochromator slitwidth of 50 μm. This means that the electron spectrometer broadening is about 0.3 eV and that the photon bandwidth is about 0.5 eV at the photon energies of the $2p_{Cl} \rightarrow \sigma^*$ resonance excitations. Some higher-resolution spectra were also taken at a pass energy of 25 eV, giving an electron spectrometer broadening of about 0.15 eV.

The kinetic energies (165–190 eV) of the Auger-type electrons emitted in the decay processes fall in the same energy range as the valence-band photoelectron and their satellite lines. Therefore the reference photoelectron spectrum was measured at a photon energy of 150 eV

[Fig. 1(c)]. This photon energy is well below any $2p_{Cl}$ resonance excitations, and the kinetic energy range (115–140 eV) of this photoelectron spectrum is free from small normal Auger peaks (around 170 eV) caused by second-order and scattered light. The shifted and normalized photoelectron spectrum was subtracted from the spectra taken at resonance energies, supposing that relative intensities of lines originating from direct photoionization do not change essentially between 150 and 200 eV photon energies. The low-kinetic-energy parts of the spectra taken at the energies of the resonance excitations also contain structures due to the normal Auger transitions originating from the ionizations of the HCl molecules by second- and higher-order diffracted light and by scattered light in the photon beam. Therefore the normal Auger spectrum taken at 275 eV photon energy [Fig. 1(b)] was also normalized and subtracted from the original resonance spectra. The shifted photoelectron [Fig. 1(c)] and normal Auger [Fig. 1(b)] spectra are depicted with the original resonance spectrum taken at 200.6 eV [Fig. 1(a)] in Fig. 1. Earlier photoabsorption measurement by Ninomiya *et al.*[6] showed two prominent maxima at photon energies of 201.5 and 202.5 eV corresponding to the $2p_{3/2}$ and $2p_{1/2}$ fine-structure components of the $2p_{Cl} \rightarrow \sigma^*$ resonance, respectively. We studied the evolution of the electron spectrum as the photon energy was tuned across these resonances. The spectra obtained with photon energies 200.6, 201.8, and 202.4 eV after subtractions of the (b) and (c) spectra of Fig. 1 are shown in Fig. 2.

CALCULATIONS

To get a more quantitative understanding of the relaxation processes of the $2p_{Cl} \rightarrow \sigma^*$ excitation in HCl, we performed multiconfigurational complete-active-space self-consistent-field[7–9] (CASSCF) calculations for the electronic ground state

$$[1\sigma^2 2\sigma^2 3\sigma^2 1\pi^4 4\sigma^2 5\sigma^2 2\pi^4 (6\sigma^*)^0]\,{}^1\Sigma^+$$

and the excited state

$$[1\sigma^2 2\sigma^2 3\sigma^1 1\pi^4 4\sigma^2 5\sigma^2 2\pi^4 (6\sigma^*)^1]\,{}^1\Sigma^+ .$$

In the CASSCF method the total orbital subspace is divided into three subspaces in such a way that the orbitals in the inactive subspace are doubly occupied in all configuration-state functions, while the secondary orbitals are empty; and in the active subspace, the electrons are distributed in all possible ways among the orbitals to

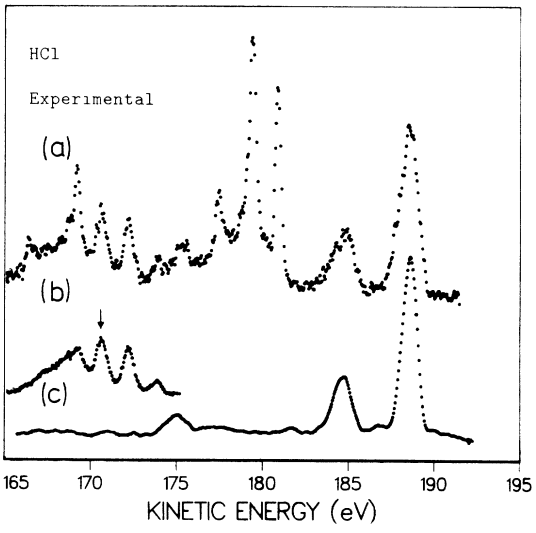

FIG. 1. (a) Electron spectrum of HCl recorded using 200.6 eV mean photon energy to excite the $2p_{Cl}$ electrons to the σ^* state, (b) the normal $L_{2,3}VV$ Auger spectrum of HCl recorded at 275 eV photon energy, and (c) the photoelectron spectrum of HCl recorded at 150 eV photon energy and shifted to the position of the photoelectron lines of spectrum *a*.

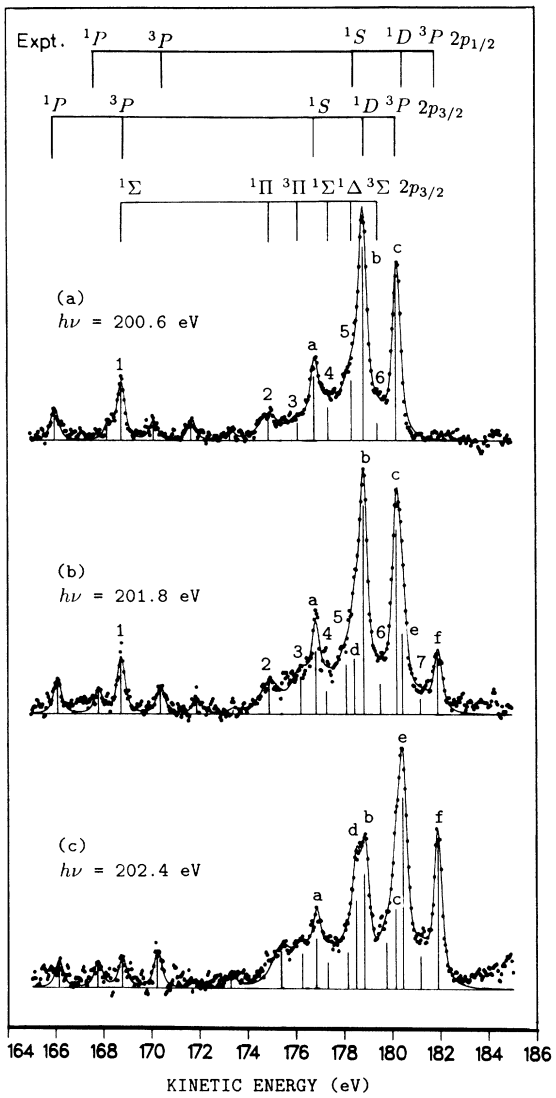

FIG. 2. Ejected electron spectra after the $2p_{Cl} \rightarrow \sigma^*$ excitations in HCl at mean photon energies of 200.6, 201.8, and 202.4 eV. The solid curves and vertical lines represent the least-squares fits of standard functions to the data points. For notations see the text.

give a complete configuration-interaction (CI) expansion within the subspace. For the ground state, the orbital space was divided in such a way that the 1σ, 2σ, 3σ, and 1π orbitals were inactive; the $4-9\sigma$, 2π, 3π, and 1δ orbitals active; and the $10-37\sigma$, $4-14\pi$, and $2-4\delta$ orbitals secondary. For the excited state a similar division of the orbital space was made; to keep the multiconfiguration (MC) expansion realistic for our computer capacity, the 4σ orbital was transferred into the inactive subspace, and the 3σ orbital, from which the excitation is assumed to be done, was transferred to the active subspace. An optimized (6*s*) Gaussian-type orbital (GTO) basis set was used for hydrogen[10] and (14*s*10*p*) for chlorine.[11] The basis set for hydrogen was contracted to the (6*s*/4*s*) contracted Gaussian-type orbital (CGTO) set and augmented with one diffuse *s*-type function and two *p*-type functions to get the final (7*s*2*p*/5*s*2*p*) basis set. For chlorine, the original GTO basis was contracted to the (10*s*8*p*) CGTO set and augmented with four *d*-type functions to get the (14*s*10*p*4*d*/10*s*8*p*4*d*) basis set. The total Mulliken gross populations of the atoms for the excited state lead to the conclusion that the dissociation process leads to a neutral excited chlorine atom in a configuration $1s^2 2s^2 p^5 3s^2 3p^6$. The calculated potential-energy curves and the allowed Franck-Condon transitions are shown in Fig. 3. The vibrational energy levels were obtained by solving the vibrational Schrödinger equation in a potential that was given as a spline fit to the computed CASSCF energies.

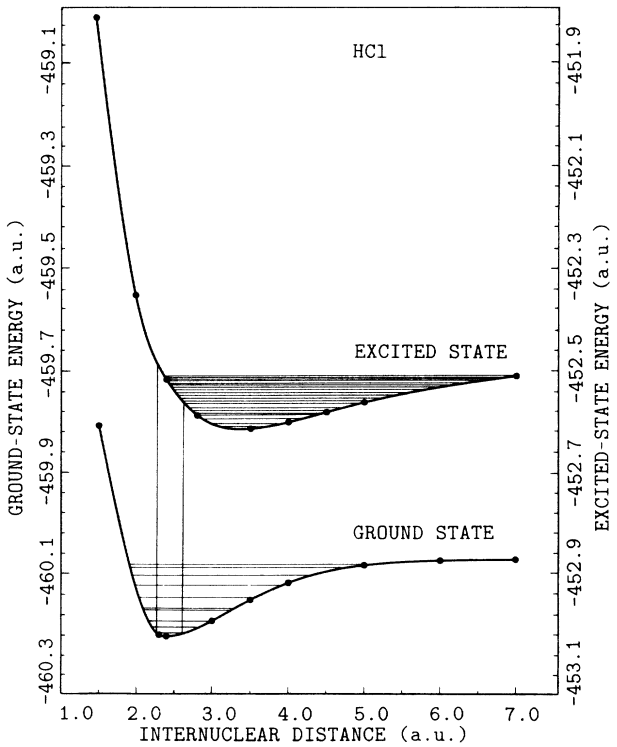

FIG. 3. Calculated CASSCF potential-energy curves for the ground state and for the excited state $[3\sigma^{-1}(6\sigma^*)^1]$ of HCl. Due to the spin-orbit splitting we have in reality separate curves for the $2p_{1/2}$ and $2p_{3/2}$ hole states, with the latter curve shifted down by 1.6 eV in the energy scale. Franck-Condon limits for electronic excitation are indicated by vertical lines.

We also carried out similar calculations of the potential curves related to some double-hole final states of the molecular Auger transition. These curves (not shown) display a pronounced local minimum similar to that in Fig. 3. At larger internuclear distances they decrease monotonically related to Coulomb explosion of the double-hole states.

The left-hand branch of the Franck-Condon transitions in Fig. 3 makes neutral dissociation of the excited $(2p)^{-1}\sigma^*$ state possible, provided that the core-hole lifetime is long enough. We studied the time evolution of this decay sequence by using a simple kinematic model. We first determined the kinetic energy E_K release during the dissociation process. Using the experimental $2p_{\mathrm{Cl},1/2} \rightarrow \sigma^*$ excitation energy of 202.4 eV [Fig. 2(c)], the dissociation energy of the neutral HCl molecule $D_0 = 4.43$ eV from Herzberg[12] and the excitation energy

$$1s^2 2s^2 2p^6 3s^2 3p^5 \rightarrow 1s^2 2s^2 2p^5 3s^2 3p^6$$

of the chlorine atom from the multiconfiguration Dirac-Fock[13] (MCDF) calculations we obtained $E_K = 202.4$ eV $-(4.43$ eV $+195.53$ eV$) = 2.44$ eV. When experimental excitation energy for atomic chlorine, determined as a sum of $E_K = 181.88$ eV of the ^3P state [see Fig. 2(a)] and the binding energy 12.97 eV from Moore's table[14] was used we obtained 0.7 eV higher kinetic energy. This difference is, however, not essential for the present purpose. For the $2p_{\mathrm{Cl},3/2} \rightarrow \sigma^*$ component at 200.6 eV photon energy [Fig. 2(a)], we found E_K to be 2.24 eV and 2.92 eV, using calculated and experimental excitation energies, respectively. Second, we determined the lifetime of the 2*p* core hole of the isoelectronic argon atom from the width 0.12 ± 0.02 eV of the LMM Auger lines.[15] This gave lifetimes varying from 2.4 to 3.3 fsec. This lifetime was used for the $2p_{\mathrm{Cl}}$ core hole in the HCl molecule to obtain an order-of-magnitude estimate for the internuclear distance at the moment of inner-hole relaxation. We assumed that the entire kinetic energy of 2.44 eV is transferred immediately after excitation to the hydrogen atom ($m_{\mathrm{Cl}}/m_{\mathrm{H}} \sim 35$). Using the classical relation between velocity and kinetic energy, the internuclear distance would then be from 3.4 to 3.8 a.u. The kinematic model used is rough and only indicates that the time scale of the dissociation is of the same order of magnitude as the time scale of the electronic decay.

After dissociation of the HCl molecule the produced excited Cl atom decays nonradiatively. To study this decay in detail, we carried out Dirac-Fock calculations for the $2p^{-1}3p^6 \rightarrow 3p^4$ Auger transition energies[13] and rates.[16] The computations were done within the single-configuration approximation. The profiles in Fig. 4 display our calculated spectrum. In Fig. 4(a) we include the $2p_{3/2}^{-1} \rightarrow 3p^{-2}$ transitions only, whereas in Figs. 4(b)–4(c) we have a weighted sum of the $2p_{3/2}^{-1} \rightarrow 3p^{-2}$ and the $2p_{1/2}^{-1} \rightarrow 3p^{-2}$ transitions with the mixing ratios (b) 60:40 and (c) 20:80, respectively.

By changing the mixing ratio of fine-structure components we simulate our measurements where the mean photon energy was tuned from the excitation of $2p_{3/2}$ towards the excitation of $2p_{1/2}$ electrons to the σ^* orbital.

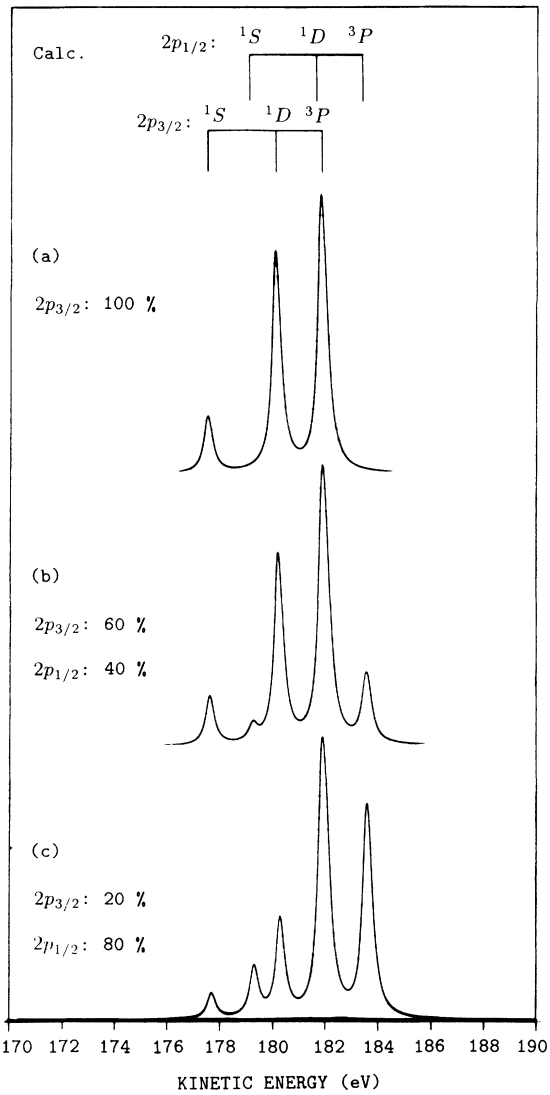

FIG. 4. The calculated $2p^{-1}3p^6 \rightarrow 3p^4$ Auger spectra of the neutral excited Cl atom.

Since the relative probability of producing atomic chlorine with $2p_{1/2}$or $2p_{3/2}$ hole states has not been evaluated by calculating the pertinent photoexcitation cross sections, a quantitative comparison of intensity ratios between our experiment (Fig. 2) and theory (Fig. 4) is not meaningful.

DISCUSSION

According to the simple kinematic consideration above, the core hole relaxes at a large internuclear distance very close to the separated-atoms limit. A comparison between experimental and calculated spectra supports this picture. The most pronounced peaks labeled $a-f$ in Fig. 2 are very well reproduced by the atomic calculations of Fig. 4. Moreover, the total Auger linewidth for peaks c and b in Fig. 2 is $\sim$ 0.2 eV, which is approximately equal to the corresponding linewidth in the isoelectronic Ar. The peaks a, b, and c in Fig. 2(a) can be assigned to the transitions from the $2p_{3/2}$ hole state to the $3p^4(^1S)$, $3p^4(^1D)$, and $3p^4(^3P)$ states. In passing from Figs. 2(a) to 2(c) three other peaks, labeled by d, e and f gain intensity, whereas the peaks a, b, and c lose intensity. Thus the peaks d, e, and f can be interpreted to the transitions from the $2p_{1/2}$ hole state to the $3p^4(^1S)$, $3p^4(^1D)$ and $3p^4(^3P)$ states. The observed energy difference of 1.6 eV between the peaks a, b, and c and the peaks d, e, and f is indeed, within the accuracy of our measurement, equal to our calculated fine-structure splitting. The dominating atomic line structure is also in agreement with our potential-energy calculations in Fig. 3, where the left-hand branch of the allowed Franck-Condon transitions populates vibrational levels in the continuum, thus leading to a fast dissociation of the molecule. Note that the sharp atomic lines indicate that when the HCl molecule is excited above the dissociation limit the dissociation takes place before the Auger decay. In the opposite case one would observe a superposition of Auger electrons emitted at various internuclear distances and giving rise to broadened and asymmetric spectral lines.

Further energy calculations for Cl predict that the $2p^{-1}3p^6 \rightarrow 3s^1 3p^5$ transitions fall in the 160–170 eV energy region. Peaks at lower kinetic energies in Fig. 2 may be caused by these transitions. We have indicated the positions of the $3s^1 3p^5\,^1P$ and ^3P states on the basis of optical data in Fig. 2.[14] Due to the strong mixing between the final-state configurations $3s^1 3p^5$ and $3s^2 3p^3 nd$ ($n = 3,4,5,\ldots$) the transitions have a very complicated peak structure. The $2p^{-1}3p^6 \rightarrow 3p^3 4p$ transitions caused by the shake-up processes $3p \rightarrow 4p$ during the Auger decay in atomic Cl are expected to appear outside the measured energy region, according to our energy calculations.

While fast neutral dissociation is clearly the most probable decay channel, the atomic peaks in Fig. 4 seem not to reproduce all the structure in the experiment. This can also be seen from the least-squares fit of Voigt functions carried out using the computer code CRUNCH,[17] which produces the lines indicated by vertical bars in Fig. 2. Besides the narrow and intense atomic peaks $a-f$, the fit yields several broad peaks 1–7, summing up to 40% of the total intensity. Some of these structures can be expected to be due to the molecular Auger decay in HCl, with the excited electron staying as a spectator. Therefore we have indicated in Fig. 2(a) some of the transitions from the $2p_{3/2}^{-1}\sigma^*$ initial state to the $5\sigma^2 2\pi^4(^1\Sigma)\sigma^*$, $5\sigma^1 2\pi^3(^1\Pi)\sigma^*$, $5\sigma^1 2\pi^3(^3\Pi)\sigma^*$ $5\sigma^2 2\pi^2(^1\Sigma)\sigma^*$, $5\sigma^2 2\pi^2(^1\Delta)\sigma^*$, and $5\sigma^2 2\pi^2(^3\Sigma)\sigma^*$ final states. The positions of these peaks have been shifted by about 8.2 eV from the normal Auger spectrum in HCl [the $2p_{3/2}^{-1} \rightarrow 5s^2 2\pi^2(^1\Delta)$ transition[18] is marked by an arrow in Fig. 1(b)] to make them coincide with some of the extra lines resulting from the fitting procedure. The shift of 8.2 eV is also fairly consistent with an observed shift of 6.6 eV between the normal and spectator Auger spectra in Ar at the $2p \rightarrow 4s$ resonance.[19] The assignment of molecular transitions in Fig. 2(a) is, however, not intended to serve as identification of separate lines but only to guide the eye to places where additional structures related to molecular decay mode could be found.

The molecular peaks can be expected to be broader

compared to the atomic ones, even though the same lifetime width due to the Auger decay may be assumed for the $2p$ core-hole states in Cl and HCl. In molecules, the transitions between different vibrational levels in initial and final state will cause the broadening of the peaks. Some of the final states may have repulsive character,[20] leading to a broadening, although even a few double-hole states displayed in our calculations local potential-energy minima. Furthermore, the electrostatic interaction between the spectator electron and the $(5\sigma 2\pi)^{-2}$ state causes extra splitting. In spite of these broadening effects a least-squares fit with one broad structureless shape for the background was not able to reproduce the spectrum in Fig. 2 as well as the fit with peaks 2–6. We were, moreover, not able to find any other atomic or molecular processes that could result in a strong background (structureless or not) observed in the experiment.

The molecular Auger transitions with the excited electron participating in the process have the same kinetic energies as the valence photoelectron lines. We did not see any dramatic change in the intensities of the main photoelectron lines at resonance, indicating that the participator Auger in HCl is of minor importance. Peak 2 in Fig. 2(a) [shifted to peak 3 in Fig. 2(b)] fits energetically with the participator process. It can hardly be distinguished from the other molecular peaks. In our previous studies[16,19,21] the participator process has also been found to be negligible. In atomic Cl it is not possible to distinguish between the spectator and participator process since the excited electron fills the $3p$ orbital where the final Auger holes also appear.

The simultaneous existence of molecular and atomic spectra is in contradiction with the model presented by Morin and Nenner for HBr.[1] The reason becomes obvious by comparing their schematic potential curves in Fig. 3 of Ref. 1 with results of our *ab initio* calculation in our Fig. 3. Due to the 2.9-eV minimum in our potential-energy curve the lowest vibrational levels of the HCl σ^* state are bound against dissociation and consequently they have a molecular decay mode. A qualitative molecular-orbital (MO) picture supporting the model of Morin and Nenner has been presented by Keller and Lefebvre-Brion.[22] Our correlated *ab initio* study based on detailed large-basis CASSCF calculation should, however, have a much higher credibility. Our result is also in agreement with basic principles of chemical bonding. The electronic state considered here has a $(2p)^{-1}(\sigma)^2(\sigma^*)^1$ configuration, i.e., two electrons in a bonding and one electron in an antibonding orbital. Thus the bond order is $\frac{1}{2}$. The experimental D_0 of HCl is 4.4 eV and the depth of the calculated excited-state well in Fig. 3 is 2.9 eV. This approximate halving is in agreement with the picture above.

Although the present molecular calculation fails to give a quantitative estimate for the interatomic potential energy, we assume that the shape of the curve is much less sensitive to the incomplete treatment of correlation. The predicted minimum in the potential energy gives a qualitative explanation for the simultaneous existence of atomic and molecular spectra. There are allowed transitions to bound vibrational states in both Franck-Condon branches in Fig. 3, which only shows one excited-state potential-energy curve with the related vibrational states. Due to the spin-orbit splitting we have in reality separate potential-energy curves for the $2p_{1/2}$ and $2p_{3/2}$ hole states, with the latter curve shifted down by 1.6 eV in the energy scale. When the excitation energy is somewhat below the $2p_{3/2}\rightarrow\sigma^*$ resonance we have only transitions belonging to the right-hand branch and therefore an enhanced molecular spectrum in comparison with the atomic component. As the beam energy approaches $2p_{3/2}$ resonance, excited states with $2p_{3/2}$ holes are allowed only in the left-hand branch giving rise to the atomic spectrum. At the same excitation energies, however, the right-hand branch becomes open for the $2p_{1/2}$ hole states leading to simultaneous existence of strong atomic and molecular lines. Note that our previous estimate of kinetic energy released in the neutral dissociation at 200.6 eV photon energy gives a positive value of 1.32 eV for the $2p_{\mathrm{Cl},1/2}\rightarrow\sigma^*$ component. The corresponding atomic Auger lines (structure f for instance) are, however, absent in Fig. 2(a). This may be due either to an inaccuracy in the evaluation of the kinetic energy or to a barrier at larger internuclear distances in the potential-energy curve. In the latter case dissociation would be possible only by tunneling and therefore the molecular Auger decay would be dominating. Unfortunately, our present calculation is not able to give a final answer if such a barrier really exists.

As the beam energy is still increased the $2p_{3/2}$ component of the spectrum fades out and also the right-hand branch related to $2p_{1/2}$ hole states becomes nearly closed. Thus we should be left with an almost pure atomic spectrum. Our experimental spectrum in Fig. 2(c) corresponds approximately to this excitation energy, but the molecular background in Fig. 2(c) is still prominent. This observation may be related to excitation of $2p_{3/2}$ electrons to Rydberg orbitals above the σ^* orbital. If the structure around atomic peak a in Fig. 2(c) is due to the decay of such states, a shift of about 6 eV is observed between normal and spectator Auger spectra in the molecule. This agrees well with the finding for Ar $4s$ excitation, which could be expected to have some resemblance to HCl $4s$ excitation.

Our present study gives only a qualitative description of the molecular decay mode. Therefore a new synchroton-radiation study covering a wider range of excitation energies around this resonance would be very informative. In fact, related to our present study we have already monitored the electron spectrum with photon energy slightly below the $2p_{3/2}$ resonance. These results indicate an enhancement of the molecular component with respect to the atomic one as predicted above. Due to the low statistics of this spectrum it is not reported here.

In conclusion we have shown that the fast neutral dissociation followed by the Auger decay of the atomic Cl fragment is the dominating decay channel of the HCl $2p_{\mathrm{Cl}}\rightarrow\sigma^*$ resonance state. As far as atomic lines are concerned, our finding supports the recent interpretation of the HBr electron spectrum by Morin and Nenner.[1] Our experimental spectrum has, however, a large background of broad structures, which cannot be explained on

the basis of atomic spectra. We have tentatively assigned this background to Franck-Condon transitions leading to bound vibrational levels of the HCl σ^* state having a nonradiative molecular decay mode.

ACKNOWLEDGMENTS

We would like to acknowledge the financial support from the National Research Council of Canada, the Natural Sciences and Engineering Research Council of Canada, the University of Western Ontario, and the Research Council for the Natural Sciences of the Academy of Finland. We would also like to acknowledge the assistance of A. Kiviniemi, and the staff at Synchrotron Radiation Center (Stoughton). We would also like to thank Professor Pekka Pyykkö for his advice concerning the excited core-hole states in diatomic molecules.

[1]P. Morin and I. Nenner, Phys. Rev. Lett. **56**, 1913 (1986).
[2]P. Morin and I. Nenner, Phys. Scr. T **17**, 171 (1987).
[3]G. G. B. de Souza, P. Morin, and I. Nenner, Phys. Rev. A **34**, 4770 (1987).
[4]B. W. Yates, K. H. Tan, L. L. Coatsworth, and G. M. Bancroft, Phys. Rev. A **31**, 1529 (1983).
[5]K. H. Tan, G. M. Bancroft, L. L. Coatsworth, and B. W. Yates, Can J. Phys. **60**, 131 (1982).
[6]K. Ninomiya, E. Ishiguro, S. Iwata, A. Mikuni, and T. Sasaki, J. Phys. B **14**, 1777 (1981).
[7]B. O. Roos, P. R. Taylor, and P. E. M. Siegbahn, Chem. Phys. **48**, 157 (1980).
[8]P. E. M. Siegbahn, A. Heiberg, B. Roos, and B. Levy, Phys. Scr. **21**, 323 (1980).
[9]P. E. M. Siegbahn, J. Almlöf, A. Heiberg, and B. Roos, J. Chem. Phys. **74**, 2384 (1981).
[10]S. Huzinaga, J. Chem. Phys. **42**, 1293 (1968).
[11]S. Huzinaga and C. Arnau, J. Chem. Phys. **21**, 207 (1980).
[12]G. Herzberg, *Spectra of Diatomic Molecules* (Van Nostrand, Princeton, 1950).
[13]I. P. Grant, B. J. McKenzie, P. H. Norrington, M. F. Mayers, and C. Pyper, Comput. Phys. Commun. **21**, 207 (1980).
[14]C. E. Moore, *Atomic Energy Levels as Derived from Analyses of Optical Spectra,* Natl. Bur. Stand. Circ. No. 467 (U.S. GPO, Washington, DC, 1949), p. 159.
[15]J. Väyrynen and S. Aksela, J. Electron Spectrosc. Relat. Phenom. **16**, 423 (1979).
[16]H. Aksela, S. Aksela, J. Tulkki, T. Åberg, G. B. Bancroft, and K. H. Tan, Phys. Rev. A **39**, 3401 (1989).
[17]C. D. Akers, C. Pathe, J. J. Barton, F. J. Grunthaner, P. J. Grunthaner, J. D. Klein, B. F. Lewis, J. M. Rayfield, R. Ritchey, R. P. Vasquez, and J. A. Wurzbach, CRUNCH *User's Manual* (California Institute of Technology, Pasadena, 1982).
[18]H. Aksela, S. Aksela, M. Hotokka, and M. Jäntti, Phys. Rev. A **28**, 287 (1983).
[19]H. Aksela, S. Aksela, H. Pulkkinen, G. M. Bancroft, and K. H. Tan, Phys. Rev. A **37**, 1798 (1988).
[20]H. J. Lempka, T. R. Passmore, and W. C. Price, Proc. R. Soc. London **304**, 53 (1968).
[21]S. Aksela, O-P. Sairanen, H. Aksela, G. M. Bancroft, and K. H. Tan, Phys. Rev. A **37**, 2934 (1988).
[22]F. Keller and H. Lefebvre-Brion, Z. Phys. D **4**, 15 (1986); Pekka Pyykkö (private communication).